JOURNAL OF GEOPHYSICAL RESEARCH, VOL. 114, A05103, doi:10.1029/2008JA013983, 2009

Experiments on dust transport in plasma to investigate the origin of the lunar horizon glow

X. Wang,[1] M. Horányi,[1,2] and S. Robertson[1]

Received 9 December 2008; revised 10 February 2009; accepted 16 March 2009; published 8 May 2009.

[1] Dust grains on the lunar surface are exposed to UV radiation and solar wind plasma and can collect electrical charges, leading to their possible lift-off and transport in the presence of near-surface electric fields. Motivated by the long-standing open questions about the physics of electrostatic lunar dust transport, we investigated the dynamics of dust grains on a conducting surface in a laboratory plasma. The dust used in these experiments was a nonconducting JSC-Mars-1 sample with particle size of less than 25 microns. We found that dust grains placed on a conducting surface, which is biased more negatively than its floating potential, charge positively, and an initial pile spreads to form a dust ring. Dust particles were observed to land on insulating blocks, indicating the height of their hopping motion. The measured electrostatic potential distribution above the dust pile shows that an outward pointing electric field near the edge of the pile is responsible for spreading the positively charged grains. A nonmonotonic potential dip was measured in the sheath above an insulating patch, indicating a localized upward electric field causing the dust lift-off from the surface. Faraday cup measurements showed that the grains near the boundary of the dust pile collect more charge than those closer to the center of the dust pile and can be more readily lifted and moved in the radial direction, leading to the formation of a spreading ring.

Citation: Wang, X., M. Horányi, and S. Robertson (2009), Experiments on dust transport in plasma to investigate the origin of the lunar horizon glow, *J. Geophys. Res.*, *114*, A05103, doi:10.1029/2008JA013983.

1. Introduction

[2] The lunar surface is exposed to solar UV radiation and solar wind plasma causing the dust to become charged. Electric fields are also created at the lunar surface due to the photoemission from the dayside [*Manka*, 1973], the differential photoelectric charging near the terminator region [*Criswell and De*, 1977; *Wang et al.*, 2007a, 2007b], and the solar wind plasma charging on the nightside [*Halekas et al.*, 2005]. In these fields, charged dust particles can possibly be lofted and transported by electrostatic forces. Several *in situ* observations of dust transport on the lunar surface have been reported. The horizon glow, observed by the Surveyor 5, 6 and 7 spacecraft, is thought to be caused by clouds of dust particles at a height of <1 m [*Rennilson and Criswell*, 1974]. The bright streamers at altitudes of ~100 km, reported by Apollo 17 astronauts in the orbiting command module, could be caused by dust leaving the lunar surface at high speeds [*McCoy and Criswell*, 1974; *Zook and McCoy*, 1991; *Stubbs et al.*, 2006]. The Lunar Ejecta and Meteorites Experiment (LEAM), deployed on the surface during the Apollo 17 mission, reported elevated dust impact rates during the passage of the sunrise and sunset terminators [*Berg et al.*, 1973, 1976]. More recently, the star tracker camera on the Clementine spacecraft also imaged a faint glow along the lunar horizon, in addition to the zodiacal light, that may be due to levitated lunar dust [*Zook et al.*, 1995].

[3] Theoretical and numerical work has been done for electrostatic transport of dust in the photoelectron sheath above surfaces in space [*Nitter et al.*, 1998; *Colwell et al.*, 2005], near the terminator of the Moon [*Borisov et al.*, 2006] as well as on asteroids [*Lee*, 1996]. The levitation of lunar regolith stimulant via electrostatic forces was experimentally studied by *Doe et al.* [1994]. The presence of dust particles has been analyzed from modification of the sheath profile [*Arnas et al.*, 2000, 2001]. The possible loss of dust from a surface exposed to plasma has also been demonstrated [*Sheridan et al.*, 1992; *Flanagan and Goree*, 2006].

[4] In our own previous experiments, dust particles in plasma were seen to lift from a surface and levitate in the sheath above it [*Sickafoose et al.*, 2002]. The observed levitation heights were successfully modeled by a collisional sheath theory [*Robertson et al.*, 2003]. Here we present experimental results on the transport of insulating dust on a conducting surface in plasma, including the temporal evolution of the distribution of the electric fields above a spreading pile of dust.

2. Experimental Setup

[5] The dust transport experiments are conducted in a cylindrical stainless steel vacuum chamber (Figure 1), that

[1]Department of Physics, University of Colorado at Boulder, Boulder, Colorado, USA.
[2]Laboratory for Atmospheric and Space Physics, University of Colorado at Boulder, Boulder, Colorado, USA.

0148-0227/09/2008JA013983$09.00

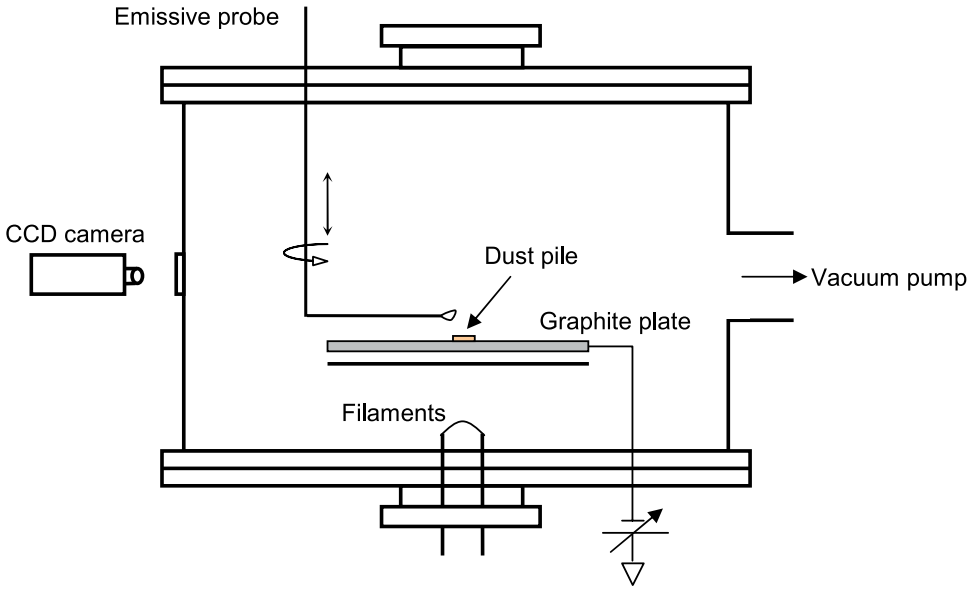

Figure 1. Experimental setup for dust transport on a surface in plasma and probe diagnostics.

is 51 cm in diameter and 28 cm high. The base pressure of the chamber is approximately 1×10^{-6} Torr. Plasma is created in argon gas of 6.0×10^{-4} Torr by electrons emitted from a negatively biased hot filament located at the bottom of the chamber. Langmuir probe data indicate that the electron density n_e is $\sim 10^8$ cm^{-3}, temperature T_e is $\sim$4 eV and the Debye length λ_{De} is $\sim$0.15 cm. JSC-Mars-1 dust simulant is used in the experiments, which is nonconducting and its mass density is 1.76 g/cm^3 [*Allen et al.*, 1998]. The dust is sieved to remove particles with size greater than 25 μm. Dust piles are placed near the center of a graphite plate, which is 22 cm in diameter. The plate surface is biased at $\Phi_0 = -60$V that gives a sheath thickness of $s \approx \lambda_{De}(\Delta\Phi/T_e)^{0.75} = 1.1$ cm, where $\Delta\Phi$ is the difference between the potential at the sheath edge and the surface bias [*Lieberman and Lichtenberg*, 1994]. When the surface is electrically isolated, the floating potential is -18 V. This large negative value is a consequence of the population of high energy electrons in the plasma. A metal plate placed between the graphite surface and the filament prevents primary electrons from being collected by the graphite surface. The spreading of dust layers are recorded by a CCD camera.

3. Dust Transport Experiments

[6] The first experiments were performed with an initial dust pile with a diameter of $\sim$0.6 cm and thickness less than 0.1 cm. The images taken before the plasma is turned on (i.e. $t = 0$ minute) and at $t = 1$, 20 and 45 minutes afterward are shown in Figure 2a. The dust particles start to spread uniformly in all directions at $t = 1$ minute. At $t = 20$ minutes, a "bull's eye"–like pattern is formed with a pile in the center surrounded by a dust "ring" with outer radius of $\sim$1 cm that is comparable to the plasma sheath thickness. At $t = 45$ minutes, the dust spreading appears to stop with a "final" configuration showing a diffuse ring.

[7] Simultaneously, measurements are made of the radial variation of the potential across the spreading dust patch from -3 to +3 cm in radius and $h = 2$ mm above the surface (Figure 2b). Data are from a motor driven emissive probe and are analyzed by the current bias method [*Diebold et al.*, 1988]. Far from the dust pile, for $\Phi_0 = -60$ V, the potential at this height is expected to be the order of $\Phi = \Phi_0\, e^{-h/s} \approx -50$ V. Insulating dust particles on a conducting surface that is biased more negative than the floating potential will charge positively, increasing the measure potential over the dust pile [*Wang et al.*, 2007a, 2007b], causing a radially outward pointing electric field that is responsible for the initial spreading of the pile. The developing potential humps at later times indicate the "bull's eye" and ring formation, respectively, which (as we show below) are due to the electric field and the charge distribution of the grains as function of their radial location.

[8] The transport of dust also involves lofting the grains above the surface. Figure 3 shows two initial dust piles resting on the graphite surface 3 mm away from a 6 mm high insulating block, and another on an insulating sheet. After the plasma is turned on, the pile on the insulating sheet does not move as expected. However, the dust pile on the graphite surface is observed to spread and dust particles accumulate on both the side and top of the insulating block. This indicates that particles on the graphite surface must be lifted off to a height of at least 6 mm above the conducting surface.

[9] To investigate the liftoff mechanism without the complication of dust spreading in time, the vertical potential distributions were measured above a thin solid insulating disc (1.1 cm in diameter), representing the dust pile. In these experiments, the electron density $n_e \sim 10^7$ cm^{-3}, temperature $T_e \sim 4$ eV, resulting in a Debye length ($\lambda_{De} \sim 0.4$ cm) ~ 3 times larger than in the previous experiments in order to obtain a more easily measured potential distribution close to insulating disc.

[10] Figure 4a shows the emissive probe scans for different bias potentials on the graphite surface, as a function of height above the center of the insulating disc. A surface bias close to the floating potential results in a monotonically decreasing plasma potential toward the surface, indicating

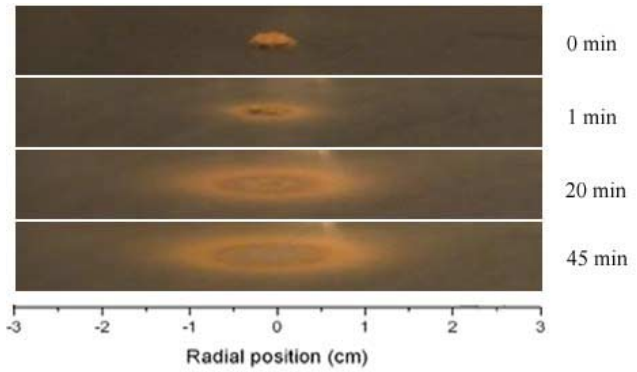

(a)

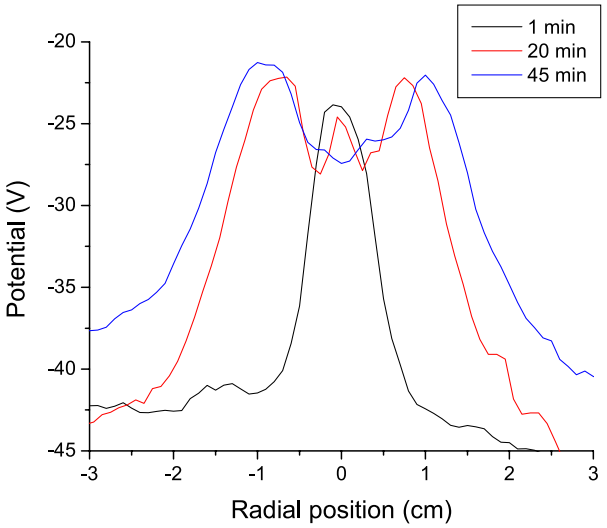

(b)

Figure 2. (a) Images of initial pile of grains with size of <25 μm at $t = 0$ minute and at $t = 1$, 20, and 45 minutes after plasma is turned on. (b) The radial potential distribution at each time step, taken 2 mm above the surface with a spatial resolution of ≈0.1 cm. The probe was swept from −3 to +3 cm through the center of the dust pile in about 5 sec. The asymmetry of the potential distribution is due to the slight slant of the probe's path.

an electric field pointing downward, as same as the direction of gravity. When the surface is biased to −60 V, a non-monotonic potential structure forms in the sheath with a minimum at 0.5–1 cm above surface. This potential dip shows an upward electric field near the insulating disc. The vertical electrostatic force acting on a positively charged grain now points upward against gravity. The depth of the potential dip is found to increase as the surface is biased more negatively. If this near-surface electric field acts on grains with sufficiently large positive charges, the electric force overcomes gravity, and the dust particles can be lifted off the surface and land in the surrounding area. A full two dimensional map of the measured potential distribution above the insulating disc with a bias voltage of −80 V is

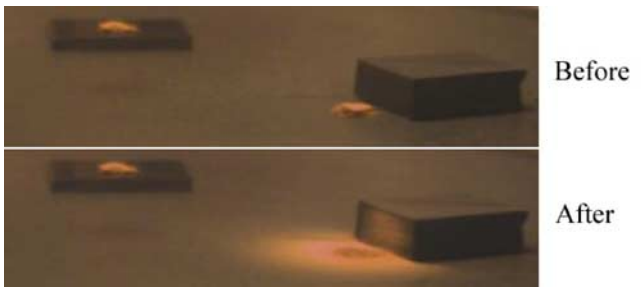

Figure 3. A dust pile resting on the graphite surface 3 mm away from a 6-mm high insulating block and another on an insulating sheet at $t = 0$ and $t = 45$ minutes after plasma is turned on.

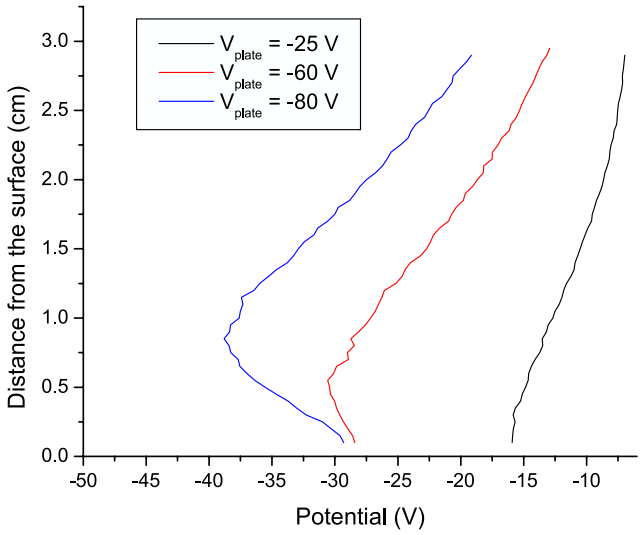

(a)

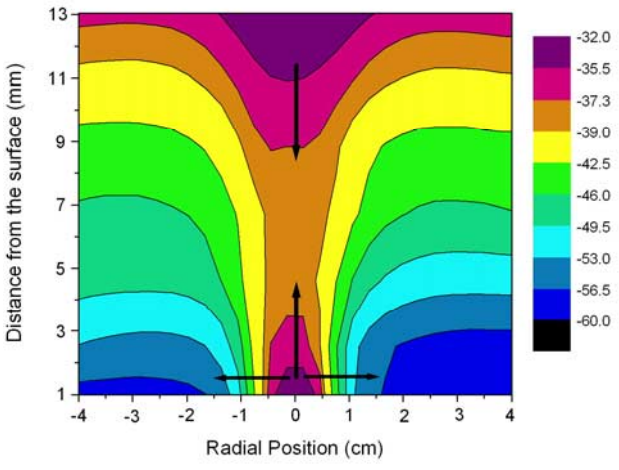

(b)

Figure 4. (a) Vertical potential distributions above the center of an insulator 1.1 cm in diameter on the surface biased at different voltages. (b) Potential contours above the insulator sitting on the surface biased at −80 V. Arrows represent electric fields.

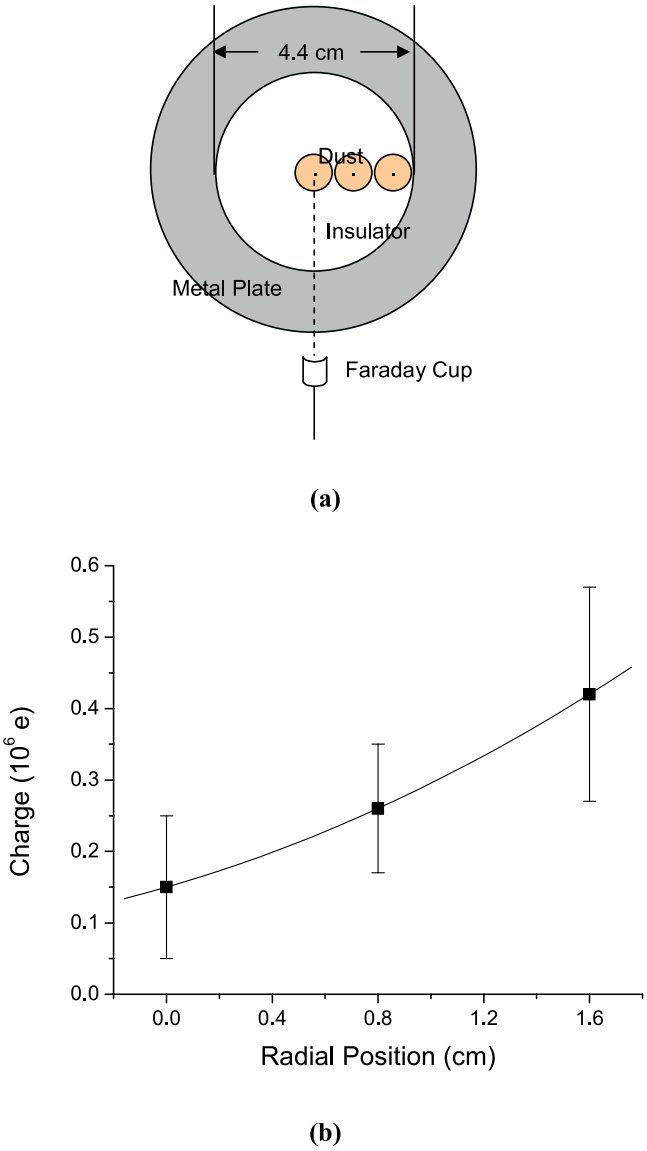

Figure 5. (a) A setup for measuring charge on dust grains as a function of distance from the center of the dust pile. (b) Charge on the dust particles that have fallen through holes in the insulating disc, as a function of location. The points are the mean of 40 measurements, and the error bars show the standard deviation.

shown in Figure 4b, indicating an electric field pointing up and radially outward near the disc, as well as a potential dip at a height of ~5 mm.

[11] The explanation for the potential profiles shown in Figures 2 and 4 is as follows. When the radius and the thickness of the dust pile are smaller than the sheath thickness of the conducting surface, the potential structure above the dust pile is mainly determined by the surface sheath. A negative potential barrier in the sheath returns most electrons to the plasma and accelerates ions toward the surface, including the dust pile. Initially, dust particles collect more ions than electrons and charge positively, building a positive potential barrier above the dust pile to equalize the electron and ion fluxes. The combination of the surface and dust pile sheaths results in a nonmonotonic potential distribution. When the surface bias increases, the dust pile collects more ions to reach this equilibrium state.

4. Dust Charge Measurements

[12] To investigate the formation of the "bull's eye" pattern, the charge on the particles as a function of distance from the center of the dust pile was measured by having the particles fall through holes into a Faraday cup. The experimental setup has been described previously [*Wang et al.*, 2007a, 2007b]. For these charge measurements the filament is moved to the side wall of the chamber so that the Faraday cup can be located below the biased surface. In this configuration the primary electrons can directly reach the surface (Figure 5a). The insulating dust pile was replaced with a 4.4 cm diameter insulating disc on which a few dust particles were placed. The disc is divided into three concentric annular regions of equal thickness and with small holes in the center of each region. JSC-Mars-1 simulant with a size of ~100 μm was used for the charge measurements in order to have a larger charge signal in the Faraday cup. The radial charge distribution was measured by moving the insulating disc to sequentially align the small holes above the Faraday cup. The surface was agitated so that the particles could move and fall through the hole. The plasma sheath thickness s is made to be ~2.6 cm by biasing the surface at −60 V ($n_e = \sim 2 \times 10^7$ cm^{-3}, $T_e = \sim 3$ eV and $\lambda_{De} = 0.3$ cm), which is comparable to the radius of the insulator disc. The floating potential of the surface is −28 V due to primary electrons with energy ~40 eV. Figure 5b shows a monotonic increase of dust charge with distance from the center of the disc. Particles near the edge have a charge approximately 3 times larger than the particles near the center.

[13] The vertical potential distributions at different radial positions above an insulating disc 4.0 cm in diameter are shown in Figure 6. The graphite surface is biased at −60 V. These scans were taken in the original experimental configuration used for the scans in Figure 4. The data show that

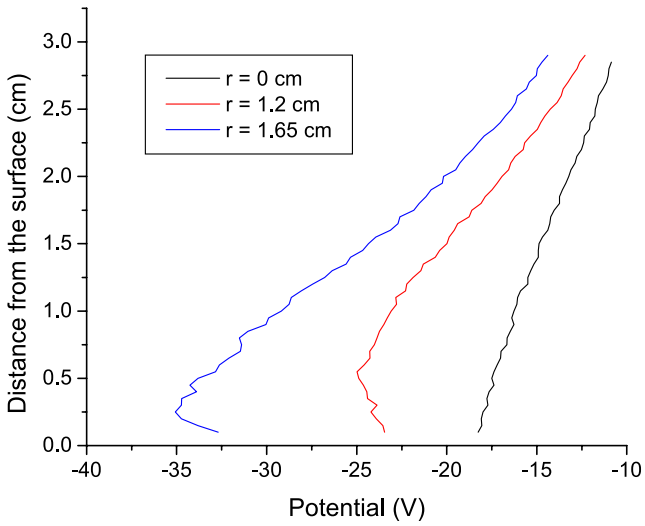

Figure 6. Vertical potential distribution at different radial positions above an insulating disc.

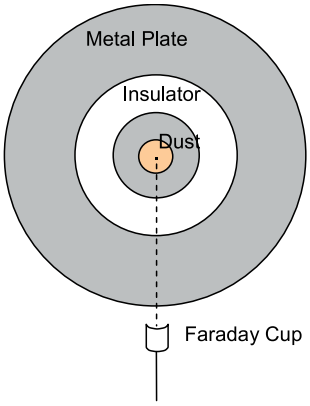

(a)

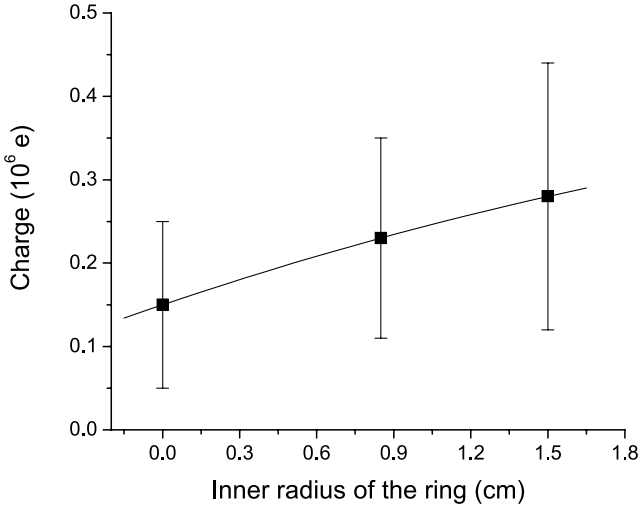

(b)

Figure 7. (a) A setup for measuring the charge on dust grains as function of the radius of a surrounding insulating ring. (b) Charge of dust particles on the insulating center as a function of the inner radius of the surrounding insulating ring.

both the depth of the potential dip, as well as the magnitude of the potential near the surface, increases in the radial direction, consistent with the increase of the measured dust charge with distance from the center. When the radius of the insulator disk is comparable to the thickness of the sheath, the effect of the surface sheath becomes reduced above the center, compared to its effect above the edge of the disk. This results in the potential falling slower at the center than at the edge. The dust particles at the center thus have to collect fewer ions and form a shallower positive potential barrier to reach equilibrium, than the particles closer to the edge of the disc.

[14] There must be a threshold at a particular radial position where the electrostatic field combined with the dust charge results in a sufficiently large force to overcome adhesion and start to move dust particles. While the particles closer to the center remain fixed, dust beyond this critical radius are transported outward, leading to the initial formation of the observed ''bull's eye'' pattern.

[15] As the dust particles continue to separate and the surrounding dust ring becomes large enough, the initially left behind central particles are observed to start spreading as well, eventually forming a single ring. This indicates that they will eventually collect sufficiently large charges to initiate transport. The effect of the increasing radius of the spreading dust ring on charging of the central dust pile was investigated using the experimental setup shown in Figure 7a. To remove the time dependence, the dust pile in the center is replaced with an insulating disc on which a few dust particles are placed, and the surrounding spreading dust ring is replaced with an insulating ring of different inner radii. Figure 7b shows that the charge on dust particles at the center increases with the inner radius of the surrounding ring. Thus, as the outer rings are getting larger, the inner region becomes exposed to the unperturbed plasma flow towards the conducting surface. The grains in the center are increasingly exposed to the same electric fields and collect similar charges as if they were near the edge of a single disc. At the same time, the potential distribution reestablishes and shows a potential hump in the center, which results in an outward electric field.

5. Summary and Discussion

[16] A circular patch of nonconducting dust particles is observed to spread on a conducting surface in a plasma when the surface is biased more negative than the plasma floating potential. The spreading dust pile forms a ''bull's eye'' pattern with an outer shell of dust moving away from a central region, where initially the dust remains stationary. As the outer ring grows, the central region also becomes mobilized, eventually forming a single dust ''ring.'' The measured radial potential distributions show (1) an outward electric field near the edge; and (2) a nonmonotonic potential dip, which indicates an upward pointing electric field near the center of the dust pile. The combination of positive grain charges, and the up and radially outward pointing electric field can lead to the spreading of the dust pile. The magnitude of both the electric field and the grain charge increases toward the edge of the pile, leading to the mobilization of dust that is farther away than a critical distance from the center. This leads to the formation of the ''bull's-eye'' pattern. As the outer shell expands beyond a distance comparable to the thickness of the sheath, its effect on the rest of the pile diminishes, and the ''left behind'' dust also starts spreading, eventually joining the earlier mobilized dust grains to form a single ring.

[17] Our experiments show that dust on a conducting surface in a plasma environment can be electrostatically transported. The efficiency of the transport is a function of the geometry of the dust layer, as well as the potential of the surface relative to the local plasma potential. Similar processes might be at work on the night side of the Moon, for example. The average solar wind speed is about 400 km/s and the typical plasma temperature is on the order of 10 eV. The flow is supersonic for the ions but remains subsonic for the electrons. To a first approximation, the electron flux initially reaching the surface near the terminators remains constant, leading to the buildup of a sufficiently large ($\sim$kV) negative surface potential. This potential reduces the electron flux and

returns the flowby ions to the surface near the terminator region, leaving an ion wake behind the Moon. The conditions near the ion wake boundary are similar to our experimental setup. A dust patch in the terminator region adjacent to the ion wake with a large negative potential is expected to be exposed to an ion rich sheath. Hence, similar dust mobilization and transport is likely to occur in the lunar terminator region as observed in our experiments.

[18] In addition to dust transport on the lunar surface, the contamination of instrument surfaces will be an issue for the planned return to the Moon. Conducting instrument housings resting on the insulating lunar surface will float to a potential that is determined by the characteristics of the construction materials, including their coefficients for secondary and photo emission. Dust resting on instrument surfaces may acquire different potentials, leading to their mobilization and transport to sensitive parts of these instruments.

[19] To understand the interaction of the lunar surface with its plasma environment, and to ensure the long-term operation of deployed optical and mechanical devices, the in situ measurements of the electron and ion densities, and energy distributions, as well as the simultaneous monitoring of the charging and liftoff of small grains from the lunar surface will be required.

[20] **Acknowledgments.** This work was supported by the NASA Interdisciplinary Exploration (IES) grant NNG06GG90G, and the Lunar Advanced Science and the Exploration Research (LASER) grant NNX08AY77G. The authors also acknowledge support as members of the NASA Lunar Science Institute's Colorado Center for Lunar Dust and Atmospheric Studies.

[21] Amitava Bhattacharjee thanks Robert L. Merlino and another reviewer for their assistance in evaluating this paper.

References

Allen, C. C., K. M. Jager, R. V. Morris, D. J. Lindstrom, M. M. Lindstrom, and J. P. Lockwood (1998), JSC MARS-1: A Martian Soil Simulant, in *Space 98, Proceedings of the Sixth International Conference and Exposition on Engineering, Construction, and Operations in Space*, edited by R. G. Galloway and S. Lokaj, p. 469, Am. Soc. of Civil Eng., Reston, VA.

Arnas, C., M. Mikikian, G. Bachet, and F. Doveil (2000), Sheath modification in the presence of dust particles, *Phys. Plasmas*, *7*, 4418–4422.

Arnas, C., M. Mikikian, and F. Doveil (2001), Micro-sphere levitation in a sheath of a low pressure continuous discharge, *Phys. Scr. T*, *89*, 163–167.

Berg, O. E., F. F. Richardson, and H. Burton (1973), Lunar ejecta and meteorites experiment, in *Apollo 17: Preliminary Science Report, NASA SP-330*, p. 16, NASA, Washington, D. C.

Berg, O. E., H. Wolf, and J. Rhee (1976), Lunar soil movement registered by the Apollo 17 cosmic dust experiment, in *Interplanetary Dust and Zodical Light*, pp. 233–237, Springer-Verlag, Heidelberg.

Borisov, N., and U. Mall (2006), Charging and motion of dust grains near the terminator of the moon, *Planet. Space Sci.*, *54*, 572–580.

Colwell, J. E., A. A. S. Gulbis, M. Horányi, and S. Robertson (2005), Dust transport in photoelectron layers and the formation of dust ponds on Eros, *Icarus*, *175*, 159–169.

Criswell, D. R., and B. R. De (1977), Intense localized charging in the lunar sunset terminator region: Supercharging at the progression of sunset, *J. Geophys. Res.*, *82*, 1005.

Diebold, D., N. Hershkowitz, A. D. Bailey III, M. H. Cho, and T. Intrator (1988), Emissive probe current bias method of measuring dc vacuum potential, *Rev. Sci. Instrum.*, *59*(2), 270–275.

Doe, S. J., O. Burns, D. Pettit, J. Blacic, and P. W. Keaton (1994), The levitation of lunar dust via electrostatic forces, in *Engineering, Construction, and Operations in Space*, pp. 907–915, Am. Soc. of Civ. Eng., New York.

Flanagan, T. M., and J. Goree (2006), Dust release from surfaces exposed to plasma, *Phys. Plasmas*, *13*(12), 123,504.

Halekas, J. S., R. P. Lin, and D. L. Mitchell (2005), Large negative lunar surface potentials in sunlight and shadow, *Geophys. Res. Lett.*, *32*, L09102, doi:10.1029/2005GL022627.

Lee, P. (1996), Dust levitation on asteroids, *Icarus*, *124*, 181–194.

Lieberman, M. A., and A. J. Lichtenberg (1994), *Principles of Plasma Discharges and Materials Processing*, Wiley, New York, p. 154.

McCoy, J. E., and D. R. Criswell (1974), Evidence for a high latitude distribution of lunar dust, *Proc. 5th Lunar Conf.*, *3*, 2991.

Manka, R. H. (1973), Plasma and potential at the lunar surface, in *Photon and Particle Interactions with Surfaces in Space*, edited by R. J. L. Grard, pp. 347–361, Reidel, Dordrecht, Holland.

Nitter, T., O. Havnes, and F. Melandsø (1998), Levitation and dynamics of charged dust in the photoelectron sheath above surfaces in space, *J. Geophys. Res.*, *103*, 6605–6620.

Rennilson, J. J., and D. R. Criswell (1974), Surveyor observations of lunar horizon glow, *The Moon*, *10*, 121–142.

Robertson, S., A. A. Sickafoose, J. Colwell, and M. Horányi (2003), Dust grain charging and levitation in a weakly collisional DC sheath, *Phys. Plasmas*, *10*, 3874–3880.

Sheridan, T. E., J. Goree, Y. T. Chiu, R. L. Rairden, and J. A. Kiessling (1992), *J. Geophys. Res.*, *97*, 2935.

Sickafoose, A. A., J. E. Colwell, M. Horányi, and S. Robertson (2002), Experimental levitation of dust grains in a plasma sheath, *J. Geophys. Res.*, *107*(A11), 1408, doi:10.1029/2002JA009347.

Stubbs, T. J., R. R. Vondrak, and W. M. Farrell (2006), A dynamic fountain model for lunar dust, *Adv. Space Res.*, *37*, 59–66.

Wang, X., J. E. Colwell, M. Horányi, and S. Robertson (2007a), Charge of dust on surfaces in plasma, *IEEE Trans. Plasma Sci.*, *35*(2), 271–279.

Wang, X., M. Horányi, Z. Sternovsky, S. Robertson, and G. E. Morfill (2007b), A laboratory model of the lunar surface potential near boundaries between sunlit and shadowed regions, *Geophys. Res. Lett.*, *34*, L16104, doi:10.1029/2007GL030766.

Zook, H. A., and J. E. McCoy (1991), Large-scale lunar horizon glow and a high altitude lunar dust exosphere, *Geophys. Res. Lett.*, *18*, 2117–2120.

Zook, H. A., A. E. Potter, and B. L. Cooper (1995), The lunar dust exosphere and Clementine lunar horizon glow, *Lunar Planet. Sci. Conf.*, *26*, 1577–1578.

M. Horányi, S. Robertson, and X. Wang, Department of Physics, University of Colorado at Boulder, Boulder, CO 80309, USA. (xu.wang@colorado.edu)